IAC-14-C1.9.8

MULTIPLE–SPACECRAFT TRANSFERS TO SUN–EARTH DISTANT RETROGRADE ORBITS FOR ASTEROID DETECTION MISSIONS

Camilla Colombo[1], Giorgio Mingotti[2], Franco Bernelli-Zazzera[1], Colin R. McInnes[2]

[1] Department of Aerospace Science and Technology, Politecnico di Milano, Milano, Italy; camilla.colombo@polimi.it
[2] Advanced Space Concepts Laboratory, University of Strathclyde, Glasgow, UK

As demonstrated by the meteorite fall in Chelyabinsk, Russia, in February 2013, also asteroids with a diameter smaller than 40 m can enter the Earth's atmosphere and cause a local damage on ground. For such small Potentially Hazardous Asteroids (PHAs) a short warning would be sufficient to have a protection plan in place on ground. However, small asteroids are difficult to be detected from ground, especially if they approach the Earth from the Sun direction, such as the Chelyabinsk object. For this reason, a multi-spacecraft mission was proposed to monitor PHAs from a telescope base orbiting on Distant Retrograde Orbits of the Sun – Earth system. This space-based system would allow increasing the warning time of asteroids incoming from the Sun direction. In this article a trade-off analysis is performed on the DRO and constellation size based on some measures of the detection capabilities. Moreover, the transfer to selected DROs from a Low Earth Orbit is designed to minimise the total Δv and time to build the constellation.

I. INTRODUCTION

The international interest towards Near Earth Objects is exponentially growing because of the awareness of the danger some asteroids or comets pose to the Earth. If a Tunguska-class or smaller Potentially Hazardous Asteroid (PHA) approaches the Earth from the Sun direction, its detection from ground is very difficult or even impossible.

Space-based PHAs observation has been proposed to integrate current detection for ground-based observation [1]. A constellation on sun-synchronous 800 km altitude Earth-centred orbits can cover 2 sr of the total sky at any time, but in opposite hemi-spheres during each half orbit [2]. The Sun exclusion zone is about 40 degrees half angle from the Sun–Earth line and the telescope must also avoid pointing too close to the Earth. LEO-based observation is the lowest cost space mission, because it does not need on-board propulsion to get into the final orbit, however orbit maintenance manoeuvres are needed. It enables high downlink data rates with a low power communication sub-system. Alternatively, spacecraft at the Sun–Earth Libration point L_2 can view the full sky except for the approximately 40 degree half angle cone centred at the Sun. It needs a capable launch vehicle, on-board propulsion and large Deep Space Network antennas for tracking and data downlink. Spacecraft at the Sun-Earth Libration point L_1 can view a smaller sky portion with respect to spacecraft at L_2, because the Earth is in front of the spacecraft and the Sun is behind, so there are two exclusion zones; however L_1 is an excellent position because all approaching asteroids may be viewed repeatedly with a good phase angle and hence with a good visual magnitude [3]. Recently, a mission was proposed on a heliocentric orbit with semi-major axis of 0.7 AU (i.e., a Venus-like orbit), from where Near Earth Objects could be observed with a smaller solar phase angle near opposition and so with higher brightness. This is the case of Sentinel mission, designed by the B612 Foundation [4]. From this orbit spacecraft can discover Atens

asteroids that spend most of their time inside 1 AU. Such a mission is more expensive, because it requires a large launch vehicle, a large on-board antenna, on-board propulsion and the use of the Deep Space Network. The major drawback of this orbit solution is the great difference in heliocentric longitude between the spacecraft and the Earth. In fact the heliocentric longitude goes from 0 to 180 degrees, making the communication difficult and hence impairing the ability to communicate imminent hazardous objects.

In a previous work by Stramacchia et al. [5], the feasibility of a spacecraft constellation for PHAs detection from a family of Distant Retrograde Orbits (DROs) in the Sun–Earth system was demonstrated. DROs extend beyond the Earth–L_1 distance; therefore, they can be selected as operational orbits for space observation of PHAs. In particular, since part of the orbit is spent in between the Earth and the Sun, spacecraft carrying visible band telescopes can cover a region of space that is usually forbidden using ground-based telescopes to monitor PHAs that may intersect the Earth from the Sun–Earth direction.

In this article we extend the study by assessing the feasibility of a multi-spacecraft constellation to be placed on a Distant Retrograde Orbit. PHAs monitoring capabilities are measured in terms of the coverage area that the constellation can ensure. Particular emphasis is put on Tunguska class asteroids, such as the Chelyabinsk meteor that reentered in Russia in February 2013 [6]. The reason is that: if a Tunguska-class or smaller Near Earth Object approaches the Earth from the Sun direction, its observation from ground is very difficult or even impossible. On the other side, DRO can offer a limited but sufficient warning time to react and prepare the population to an impact with local effects on ground [7].

In Ref. [5] the complete map of periodic orbits was built. Four families of simple periodic orbits – named *a*, *c*, *f* and *g* [8] – around the Earth and the L_1 and L_2 libration points were studied. Here the focus is on family *f*-orbits, alias DROs. Differential correction, coupled with numerical continuation, is employed to refine the orbits in the Sun–Earth planar Circular Restricted Three–Body Problem (CR3BP).

Then, the transfers to DROs are designed. DROs offer a stable behaviour in the framework of the CR3BPs, also in the problem at hand, the Sun–Earth one. In literature, several transfer techniques can be found: from trajectories that exploit impulsive manoeuvres through to low-thrust arcs [9],[10]. These methodologies are known as *classic transfers*. On the other hand, the so called *extended transfers* are based on the dynamical systems theory to further investigate the motion behaviour around the collinear unstable libration points of the CR3BP [11]. This way the transfer trajectories are designed exploiting the invariant manifold structure of the motion [12].

In this work, a preliminary assessment on the transfer topology was performed with respect to the size of the DROs of interest. In case of small DROs, transfers exploiting the stable manifolds of intermediate periodic orbits – tangent to the target DRO – are envisaged. The intermediate orbits are planar orbits around L_1 and L_2, (i.e., *a*–family and *c*–family as named by Hénon [8]) and simple-periodic prograde orbits (*g*–family). When large DROs are of interest, transit trajectories making use of the stable and unstable manifold structure may be investigated. In order to improve the transfer performances, an optional use of lunar gravity assist can be included, in the framework of the Moon-perturbed Sun–Earth CR3BP.

As a constellation of multiple spacecraft is studied, different strategies are here adopted to deploy properly all the spacecraft: on the one hand, they follow the same trajectory to the target DRO, but with a time delay; on the other hand, they share the same starting location but fly along different paths.

Finally, a trade-off analysis on the DRO amplitude and the number of spacecraft in the constellation and the transfer cost is performed, some measures are defined to assess the detection capabilities of the corresponding space-based system and to compare it with the one of an Earth-based system. In particular, is demonstrated that a space-based PHAs detection system allows monitoring a wide zone between the Earth and the Sun. Such area is forbidden for Earth-based telescopes. This allow the selection of the operational orbit for a multiple telescope network system for PHAs detection.

The paper is organised as follows: in Section II the dynamical model used is described, namely the Circular Restricted Three Body Problem and the Hill's problem. Then, Section III describes the peculiarities of Distant Retrograde Orbits. The detection model for assessing the minimum asteroid size to be detected from a point in space with a telescope is described in Section IV, together with the definition of the coverage area and other measures for assessing the constellation capabilities. Transfer to a selected number of DROs are designed and presented in Section V. Strategies for building a multi-spacecraft constellation for the monitoring of Tunguska class asteroids are presented. The orbit was selected among the DRO family [5] and transfer for a 2- 3- and 4-spacecraft constellation are computed. Conclusions and summary of future work is presented in Section VI.

II. RESTRICTED THREE-BODY PROBLEM AND HILL'S PROBLEM

As our interest is to investigate PHAs detection from a space-based system placed on orbit in formation with the Earth, the dynamical model used for the orbit and trajectory design is the CR3BP of the Sun and the Earth-Moon barycentre. We further restrict the motion of the spacecraft to be in the orbital plane defined by the two primaries. In what follow, we will consider three different systems of reference, the synodic system, the inertial system and Hill's system. The Synodic system rotates with constant angular velocity around the centre of mass of Sun m_1 and Earth – Moon barycentre m_2 such that the x axis is always pointing at the Sun-Earth direction. x and y are the coordinates in the synodic rotating system. The synodic system is adimensionalised with units of length equal to $r_0 = 1\,\mathrm{AU}$, unit of time equal to $\tau_0 = \sqrt{AU^3 / \left(\mu_{\mathrm{Sun}} + \mu_{\mathrm{Earth}} + \mu_{\mathrm{Moon}}\right)}$, and unit of velocity equal to $v_0 = r_0 / \tau_0$. If we introduce the mass parameter for the planetary system $\mu = m_2 / \left(m_1 + m_2\right)$, the normalised absolute position of the primary bodies in the Synodic system can be defined as $x_1 = -\mu$ and $x_2 = 1 - \mu$. The motion of the spacecraft in the field of PCR3BP is described by the system [13],[14]:

$$\begin{cases} \ddot{x} - 2n\dot{y} = \dfrac{\partial \bar{\Omega}(x,y)}{\partial x} \\ \ddot{y} + 2n\dot{x} = \dfrac{\partial \bar{\Omega}(x,y)}{\partial y} \end{cases} \tag{1}$$

where $n = 1$ is the normalised angular velocity of the Synodic system with respect to the inertial system and $\bar{\Omega}(x,y)$ is the pseudo-potential composed by the centrifugal potential and gravitational potential as:

$$\bar{\Omega}(x,y) = \frac{1}{2} n^2 \left(x^2 + y^2\right) + \frac{1-\mu}{r_1} + \frac{\mu}{r_2} \tag{2}$$

with r_1 and r_2 the distances of the spacecraft from m_1 and m_2, respectively. The scalar field in Eq. (2) influences the equations of motion through its gradient, so we can introduce in its expression a constant term that allows obtaining a more symmetric form [14]:

$$\Omega(x,y) = \bar{\Omega}(x,y) + \frac{1}{2}(1-\mu)\mu$$

Eqs. (1) have an integral of motion, the Jacobi integral that expresses the conservation of energy in the relative motion of the spacecraft.

$$J\left(x,y,\dot{x},\dot{y}\right)=-\left(\dot{x}^2+\dot{y}^2\right)+n^2\left(x^2+y^2\right)+2\left(\frac{1-\mu}{r_1}+\frac{\mu}{r_2}\right)+\left(1-\mu\right)\mu$$

In the special case of spacecraft' orbits near the secondary mass and for planetary systems with μ very small, the CR3BP can be further simplified to the Hill's problem for μ that tends to zero [14]. Through a translation to the secondary body, a change of variables and the computation of the limit $\mu\to 0$, Eq. (1) transformed to [5]:

$$\begin{cases}\ddot{\xi}-2n\dot{\eta}=3\xi-\dfrac{\xi}{\left(\xi^2+\eta^2\right)^{3/2}}=\dfrac{\partial\Omega_H\left(\xi,\eta\right)}{\partial\xi}\\ \ddot{\eta}+2n\dot{\xi}=-\dfrac{\eta}{\left(\xi^2+\eta^2\right)^{3/2}}=\dfrac{\partial\Omega_H\left(\xi,\eta\right)}{\partial\eta}\end{cases}$$

with the associated pseudo-potential function

$$\Omega_H\left(\xi,\eta\right)=\frac{1}{2}\left(3\xi^2+\frac{2}{\left(\xi^2+\eta^2\right)^{1/2}}\right)$$

while the Jacobi integral for the Hill system is

$$\Gamma\left(\xi,\eta,\dot{\xi},\dot{\eta}\right)=-\left(\dot{\xi}^2+\dot{\eta}^2\right)+3\xi^2+\frac{2}{\left(\xi^2+\eta^2\right)^{1/2}}$$

III. DISTANT RETROGRADE ORBITS

Among the families of simple-periodic orbits in the PCRTBP, family-*f* orbits first studied by Hénon [8], were proposed to monitor asteroids that may intersect the Earth on a trajectory that comes from the Sun-Earth direction [7],[5]. Family-*f* orbits are linearly stable, retrograde orbits around the second body, also called Distant Retrograde Orbits. They extend beyond the L_1 point of the Sun–Earth system, thus they would allow increasing the warning time before a possible re-entry in the Earth's atmosphere with respect to current Earth-based observation.

The initial conditions determined by Hénon in the Hill's problem [8] were refined with a differential correction method coupled with a continuation method on the orbit amplitude (i.e., energy). Each orbit is then reproduced in the CR3BP dynamics, considering, this time, a finite mass parameter $\mu=3.0404234^{-6}$ of the Sun–Earth+Moon system [5]. Fig. 1 represents the family-*f* of DROs in the CRTBP dynamics.

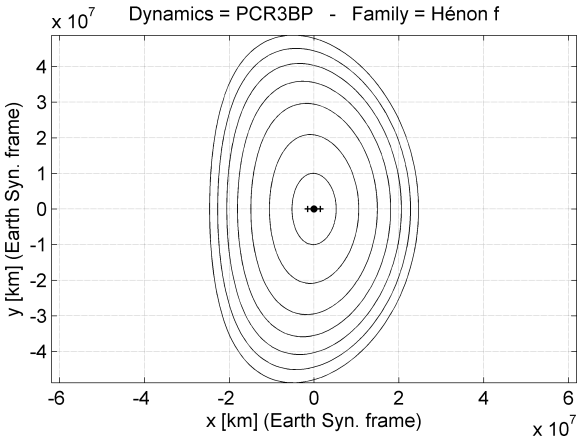

Fig. 1: Distant retrograde orbit family in the Earth-cantered synodic system. The three markers are (from left to right) L_1, the Earth and L_2.

DROs can be extended to $\Gamma\to\pm\infty$; however, orbits with a maximum distance from Earth greater than $5\cdot10^7$ km will increasingly feel the gravitational effect of the other planets (e.g., Jupiter and Venus) here not taken into account [11]. For this reason, a limit on the maximum distance from Earth of $5\cdot10^7$ km was here considered, which correspond to $\xi_0\geq-12$. Therefore, the orbit with the highest feasible energy (J = 2.9689) correspond to a period of 365.10 days, minimum and maximum velocity of 5.2514 km/s and 11.013 km/s, minimum and maximum distances from Earth of $2.6264\cdot10^7$ km and $5.2447\cdot10^7$ km, respectively. In a previous work [5] DROs were selected among other families of planar orbits as the showed to be the most favourable orbit family to obtain large distances from Earth, and consequently, good and different conditions for observation and monitoring of PHAs. Indeed family-*f* orbits have a characteristic

dimension (i.e., minimum distance from the Earth) that is larger than the Earth-L_2 distance. A spacecraft orbiting on a DRO, flies around the Sun, but in formation with the Earth, such that the spacecraft's orbit looks as a quasi-ellipse around the Earth in a Synodic system (see Fig. 1).

IV. NEAR EARTH OBJECTS DETECTION

IV.I. Asteroid detectable size

As a measure of PHAs detection capabilities from a given orbit or from an Earth base, we can compute the minimum asteroid diameter that can be observed from a point in space, considering current telescope technologies. One of the challenges when observing asteroids, is their rapid and drastic variations in magnitude. The magnitude of an object depends on its physical parameters such as the size (i.e., the diameter D) and albedo, but also on the distances to the Sun $R_1(t)$ and the observer $R_2(t)$, and the phase angle $\kappa(t)$, which is the angle between the light incident onto the observed object and the light reflected from the object (in the context of astronomical observations this is usually the angle illuminator-object-observer). The apparent magnitude or visual magnitude V is a measure of the object brightness as seen by an observer, adjusted to the value it would be in the absence of the atmosphere. V can be computed as [15]:

$$V = H + 5\log_{10}\left(R_1(t)R_2(t)\right) + \\ -2.5\log_{10}\left(\left(1-G\right)\Phi_1\left(\kappa(t)\right) + G\Phi_2\left(\kappa(t)\right)\right) \quad (3)$$

where H is the object absolute magnitude, a measure of the intrinsic brightness of a celestial body. H is defined as the apparent magnitude that the asteroid would have if it were at 1 AU from both the Sun and the observer at zero solar phase angle. $\Phi_1\left(\kappa(t)\right) = \exp\left[-3.33\left(\tan\frac{\kappa}{2}\right)^{0.63}\right]$ and $\Phi_2\left(\kappa(t)\right) = \exp\left[-1.87\left(\tan\frac{\kappa}{2}\right)^{1.22}\right]$ are two phase functions that describe the single and multiple scattering of the asteroid's surface. In Eq. (3), $R_1(t)$ and $R_2(t)$ are expressed in AU. The phase slope parameter G describes how the asteroid brightness falls with increasing solar phase angle. $G = 0.15$ was considered, corresponding to a low-albedo for C-type asteroids [16]. The model in Eq. (4) was previously used by Sanchez and Colombo to assess the time required for detecting PHAs from an Earth and near-Earth telescope network [17].

If we assume a limiting visual magnitude $V_{\lim}$ below which asteroids can be detected, the limiting absolute magnitude $H_{\lim}$ at each time can be obtained from Eq. (3). As the asteroid move around the Sun, the smallest asteroid size $D_{\min}$ that can be detected from a given orbit (i.e., the orbit of the Earth for ground-based survey or the spacecraft's orbit for space-based survey) as a function of time, can be obtained as in Ref. [17].

$$D_{\min}(t) = \frac{1}{\sqrt{p_v}} \cdot 1329 \cdot 10^{-H_{lim}(t)/5} \quad [\text{km}] \quad (4)$$

Eq. (4) consider an *a priori* assumption on the albedo of the object that was taken equal to $p_v = 0.154$.

IV.II. Earth and space-based detection

Eq. (4) can be used to assess the capabilities of an Earth-based or a space-based PHAs detection system. Depending on the definition of the observer, the phase angle $\kappa(t)$ is the Sun-asteroid-Earth or Sun-asteroid-spacecraft angle; $R_2(t)$ is the distances in AU of the asteroid to the Earth, for ground-based survey systems, or to the spacecraft, for space-based survey systems. $V_{lim} = 23$ was set as the limiting visual magnitude for space-based survey, while $V_{lim} = 24$ as the limiting visual magnitude for ground-based survey, which corresponds to the capability of the Pan-STARRS, the Panoramic Survey

Telescope & Rapid Response System developed at the University of Hawaii's Institute for Astronomy [18].

The apparent magnitude V in Eq. (3) takes into account a full sky coverage, but in reality the sky coverage of an asteroid survey by ground telescopes is limited to the night side of the Earth, and to relatively large solar elongation. In fact an asteroid cannot be observed from ground if its direction is close to the direction of the Sun. Eq. (3) via the phase functions $\Phi_1(t)$ and $\Phi_2(t)$ has the effect of increasing the apparent magnitude and so decreasing the brightness of the asteroid. If the phase angle $\kappa(t)$ increases and approaches 180°, the visual magnitude V increases towards infinity and so this decreases the brightness of the asteroid.

Stramacchia et al. [5] compared Earth-based and space-based PHAs detection capabilities by constructing contour lines of Eq. (4) that represent the minimum asteroid size that can be observed if we have a precise geometrical configuration between the observer (i.e., Earth or spacecraft), the Sun and the asteroids. As previously done in Ref. [17], a search grid in the Earth-centred Synodic system is considered with boundaries of ± 0.5 AU, with Earth at the origin of this reference frame and the Sun at -1 AU. Set a 1000 point on the grid (x, y), which represents a PHA, the distance from the Sun can be defined as:

$$\mathbf{R}_1(t) = \begin{bmatrix} x + r_0 \\ y \end{bmatrix}$$

The distance from the Earth based observer is:

$$\mathbf{R}_{2,\,\text{Earth}}(t) = \begin{bmatrix} x \\ y \end{bmatrix}$$

while the distance from the space observer, based at $\left[x_{\text{s/c}}(t) \quad y_{\text{s/c}}(t)\right]^T$ from Earth, is

$$\mathbf{R}_{2,\,\text{space}}(t) = \begin{bmatrix} x - x_{\text{s/c}}(t) \\ y - y_{\text{s/c}}(t) \end{bmatrix}$$

The phase angle $\kappa(t)$ is then computed from the Carnot theorem as:

$$\cos\kappa(t) = \left(R_1^2(t) + R_2^2(t) - R_3^2(t)\right) \Big/ \left(2R_1(t)R_2(t)\right)$$

where $R_3(t)$ is the distance from the Sun to the observer (i.e., the spacecraft or the Earth).

For each point of the grid, the minimum detectable size from Earth $D_{\text{min, Earth}}(x, y)$ and from space $D_{\text{min, space}}(x, y)$ is computed from Eq. (4). However, some boundaries need to be defined beyond which no asteroid can be observed. Indeed, Earth-based systems have a Sun exclusion zone of about 40 degrees half angle from the Sun–Earth line and the telescope must also avoid pointing too close to the Earth [16]. For this reason, if the asteroid is within such region, the detectable diameter is set to zero. Now, fixing the minimum asteroid size we want to detect, the capabilities of an Earth-based survey system can be measured by computing the area of the region of Space which is enclosed by the level curve at $\overline{D}_{\text{min}}$ defined as $A_{\text{coverage, Earth}}$ [5]. Since the surface $D_{\text{min, Earth}}(x, y)$ is defined numerically over the (x, y) grid, the contour line $D_{\text{min, Earth}}(x, y) = \overline{D}$ is numerically found; then the area of the polygons defined by the contour line is computed to get $A_{\text{coverage, Earth}}$. Fig. 2 represents the capabilities of Pan-STARRS discovery search programs in terms of minimum diameter of the asteroid to be detected ($V_{\text{lim}} = 24.0$ is considered [1]). The black line represents the threshold for detecting an asteroid of 25 metres diameter, while the yellow area represent the coverage area $A_{\text{coverage, Earth}}$ we defined.

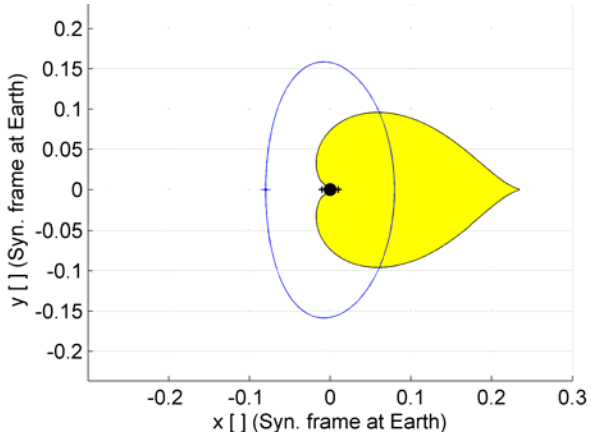

Fig. 2: Coverage area for Earth based system.

The advantage of a space-based detection from DROs is that, if a constellation is employed, visibility can be ensured also in the case a PHA it is coming from the direction away from the Sun (i.e., from the –*x* axis). For this, it is required that at least one spacecraft of the constellation is always orbiting in the inferior conjunction position [7],[5]. It is then useful to consider for each instant of time, the temporal evolution of the space-based coverage area, which depends on the instantaneous position of the spacecraft on its orbit. The spatial envelope of a multi-spacecraft constellation for different time intervals from 0 to T (i.e., the orbit period) was computed using the same numerical procedure for Earth-based observation [5]. The only difference is that this time the contour line $D_{\text{min, space}}(x,y)=\bar{D}$ is constructed from the envelope of the contour line of each spacecraft in the constellation at time t. The evolution of the spatial envelope is symmetric with respect to the orbital period, which is the time configurations obtained within the first half-period can be obtained in reverse order in the second half of the orbit period. Similarly to the Earth-based system the coverage area of the Space based system $A_{\text{coverage, space}}(t)$ can be computed.

Fig. 3 clarifies the definition of the spatial envelope (green area). Fig. 3 also shows the gained monitoring area within the exclusion zone for Earth-based systems (red area), named $A_{\text{exclusion zone, space}}(t)$. Asteroid performing close encounters with the Earth which enter this zone cannot be tracked from Earth. This was the case of the Chelyabinsk meteor.

We would like to remind that the coverage area for the constellation is function of time, its behaviour was analysed in Ref. [5], here we only consider the nominal spacecraft configuration, when one spacecraft is at the inferior conjunction and the other $n-1$ spacecraft of the constellation are equally spaced in time of T/n, where T is the orbit period.

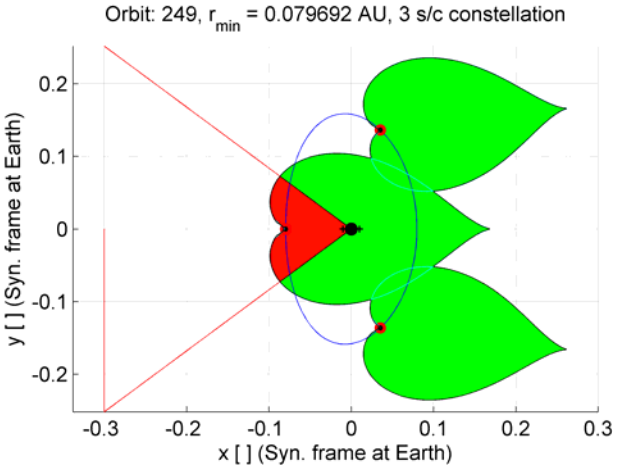

a)

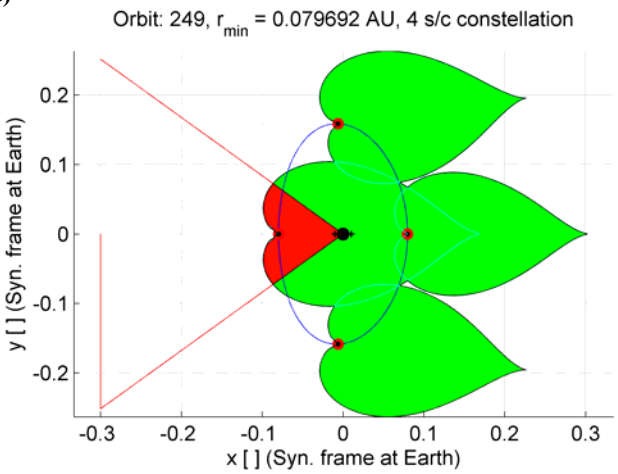

b)

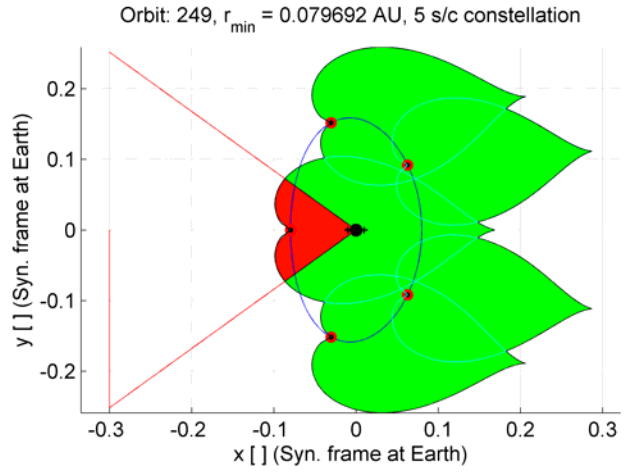

c)

Fig. 3: Coverage area for space-based system: a) 3-s/c constellation, b) 4 s/c-constellation and c) 5-s/c constellation.

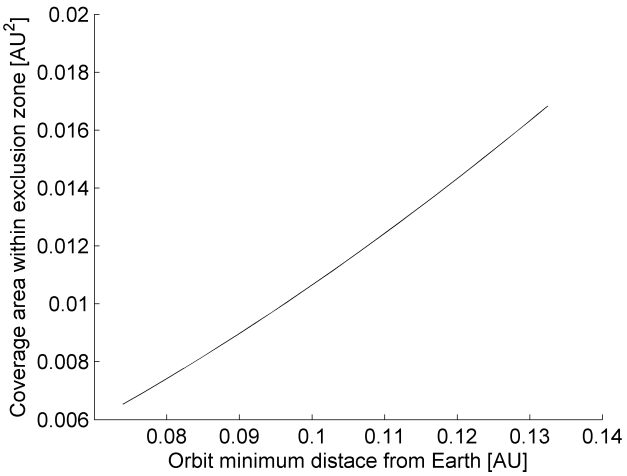

Fig. 5: Coverage area within the forbidden region as function of the constellation and orbit size.

IV.III. Constellation performances

The aim of this work is to analyse the performances of different constellation sizes and orbit amplitudes. Therefore, we take $A_{\text{exclusion zone, space}}(t)$ and $A_{\text{coverage, space}}(t)$ as measures of the constellation performances. The result is represented in Fig. 4 and Fig. 5.

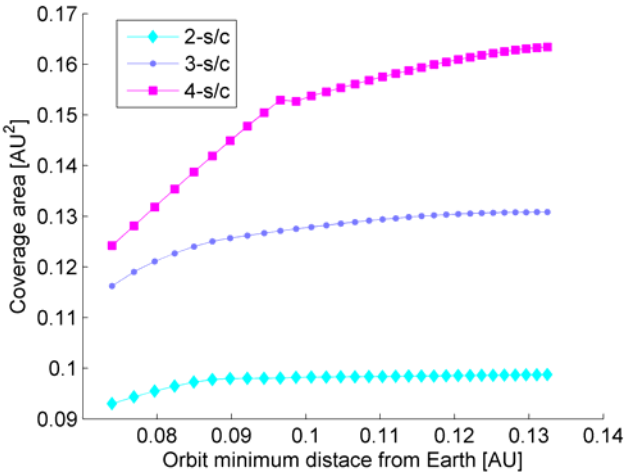

Fig. 4: Coverage area as function of the constellation and orbit size.

As expected the coverage area and the coverage within the exclusion zone increases as the number of spacecraft increases. It is expected that they both reach an asymptotic limit as the number of spacecraft increases. In any case no more than 5 spacecraft were considered here, to limit the cost of the overall mission. The larger the operational orbit, the more the coverage area is disconnected, allowing "holes" in the monitored Space (see Fig. 6). However, the advantage lie in the higher warning time if an asteroid is monitored at the inferior conjunction of an orbit with higher amplitude. The coverage area within the forbidden region increases with the orbit size. No dependence is shown with respect to the spacecraft number. The reason is that only the initial configuration is here analysed, when one spacecraft is at the inferior conjunction. However, this coverage zone changes with time, as the spacecraft moves along the orbit. For this reason, further work will compute the average of the coverage area within the exclusion zone.

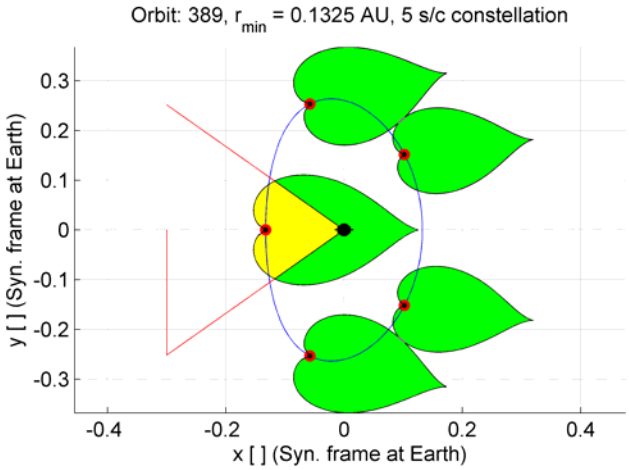

Fig. 6: Disconnected coverage area for space-based system: 5-s/c constellation, DRO with 0.1325 AU minimum distance from Earth.

V. TRANSFER TO DISTANT RETROGRADE ORBITS

V.I. Transfer design

In light of the size of the DROs that are appealing for PHAs detection [5], the *extended transfer* strategy proposed in [11] reveals to be inefficient. As there is no tangential condition between the intermediate periodic orbits belonging to the *a*-, c- and *g*-families with the ones belonging to the *f*-family that of interest in this work, the transfer strategy exploiting the invariant manifold technique requires an additional intermediate manoeuvre. This way, the transfer performances decrease as the flight time becomes longer and the overall impulsive manoeuvres magnitude becomes higher.

Therefore a *hybrid transfer* technique is proposed in this paper, where preliminary insights into the heliocentric two-body formulation of the problem are later on translated into the Sun–Earth CR3BP. Moreover, almost all the DROs of interest in this paper have a synodic period in the CR3BP frame that is very close to 1 terrestrial year [5].

In other words, when the DROs are analysed in the heliocentric inertial frame, their semi-major axis values are almost like the Earth's orbit one, with different – larger – values of eccentricity. This way, the generalised Lambert solution is assumed as first-guess looking for the minimum Δv transfer between two elliptical orbits around the Sun.

In detail, as preliminary first-guess solution in the heliocentric inertial frame, the bi-elliptic transfer arc (offering the minimum Δv cost) is assumed. Moreover, in the multi spacecraft mission scenario, the other n-1 first-guess trajectories are defined by a continuation of the bi-elliptic transfer.

V.II. Single spacecraft transfer

Once the transfer strategy to DROs is selected and first-guess solutions are generated, the optimisation process, in this paper, is performed using a direct-shooting numerical technique [20].

Considering a range of DROs with different sizes, the single spacecraft optimisation problem - based on bi-impulsive transfers - is stated according to the following key specifications.

- Initial state: the spacecraft is orbiting the Earth on a planar 167 km altitude LEO.
- Final state: the spacecraft enters the prescribed DRO, according to mission requirements.
- Performance index: the sum of the departure Δv and insertion Δv .

The dynamical model exploited in the optimisation phase is the Sun–Earth CR3BP.

V.III. Multi spacecraft transfer

As a constellation of n spacecraft - equally spaced in time - is studied, the problem of finding promising first-guess solutions becomes harder to investigate in the framework of the Sun–Earth CR3BP that is a rotating reference frame. In detail, an additional constraint on the time is included in the problem formulation.

Firstly, all the spacecraft are assumed to be at the same location on the parking LEO - at the initial time - each of them equipped with same propulsion system. The final time-spacing between each of the *n* spacecraft on the selected DRO is a function of the following three factors.

- The time spent on the LEO before the departure manoeuvre (for each spacecraft) $\Delta\tau_i$.
- The actual transfer time (for each spacecraft) ΔT_i .
- The insertion time-coordinate along the target DRO, measured from a unique location (for each spacecraft) $\Delta\varphi_i$ (this variable goes from 0 to the orbital period *T*).

As for the previous mission scenario, an optimal control problem – considering bi-impulsive transfers – is formulated according to the following key specifications.

- Initial state: the spacecraft are all orbiting the Earth on a planar 167 km altitude LEO.
- Final state: the spacecraft enter the prescribed DRO, according to mission requirements.
- Performance index: the sum of the departure Δv and insertion Δv , for all the *n* spacecraft.

For each spacecraft the constraint needs to be satisfied:

$$\Delta\tau_i + \Delta T_i + \Delta\varphi_i = T/n \qquad \forall i = 1...,n$$

Again, the dynamical model exploited in the optimisation phase is the Sun–Earth CR3BP.

V.IV. Results

For the single spacecraft transfer scenario, minimum Δv trajectories are computed. Fig. 7 represents the optimal transfer to DROs of increasing dimensions.

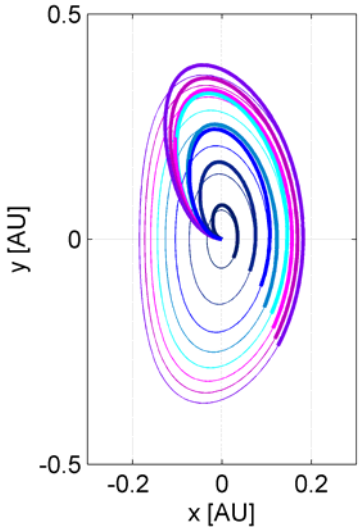

Fig. 7: Single spacecraft transfer to transfer to DROs of increasing dimensions.

In details, Fig. 8 and Fig. 9 present the behaviour of the impulsive manoeuvre magnitude and transfer time, for the optimised transfer trajectories, as a function of the DROs semi-minor axis. It can be seen that both Δv and Δt increases monotonically with the size of the DROs.

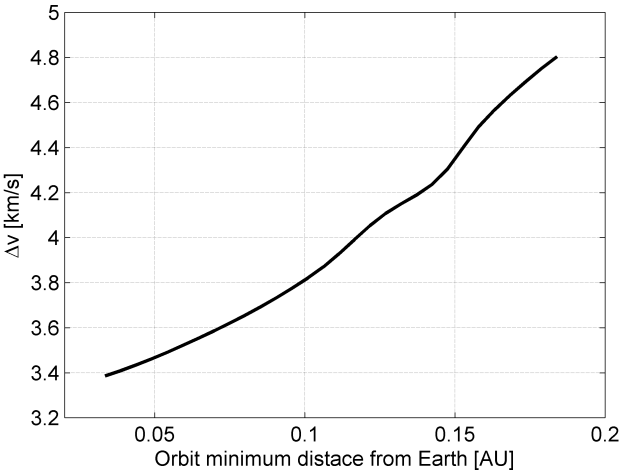

Fig. 8: Single spacecraft scenario: transfer Δv as a function of the DROs size.

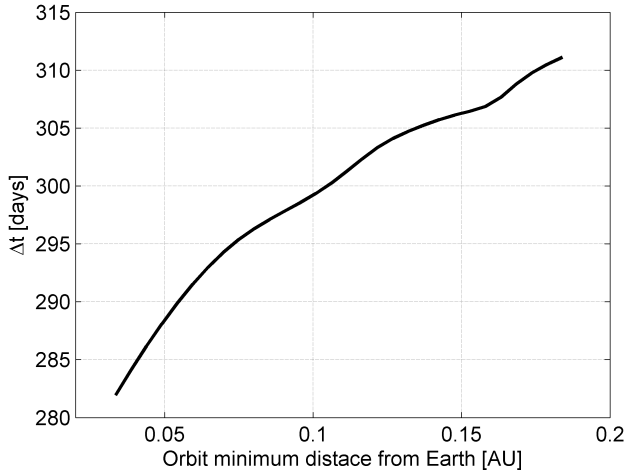

Fig. 9: Single spacecraft scenario: transfer Δt as a function of the DROs size.

As for the multi spacecraft scenario, three different options have been assumed: constellation with 2, 3 and 4 spacecraft, respectively. Moreover, the DRO with amplitude 0.07969 AU, which corresponds to 1.1921793 km was selected [5].

For each of the three mission scenarios, different transfer sequences can be exploited as a combination of basic trajectories: from solutions that envisage transfers with the same entry point into the target DRO, but at different time, through to solutions with the same flight time, but different path and entry location.

Table 1 and Fig. 10 summarise the sequence performances for multi spacecraft scenarios with $n = 2$. The Δv is the sum of all spacecraft Δv and the Δt corresponds to the arrival time of the last spacecraft, enabling the effective activation of the constellation:

$$\Delta t = t_{\text{final},i} - t_0$$
$$t_{\text{final},i} = t_0 + \Delta\tau_i + \Delta T_i \qquad i = 1,\ldots,n$$

Transfer sequence 'C' outperforms all the others in terms of total Δv (but it is the slowest), while transfer sequence 'A' is the fastest (but it is the most expensive in terms in terms of Δv).

Table 2 and Fig. 11 summarise the sequence performances for multi spacecraft scenarios with $n = 3$. Again, the Δv is the sum of all spacecraft Δv and the Δt corresponds to the arrival time of the last spacecraft, enabling the effective activation of the constellation. Transfer sequence 'D' outperforms all the others in terms of total Δv , transfer sequence 'A' is the fastest, while transfer sequence 'F' is both the most expensive and the slowest.

Table 3 and Fig. 12 summarise the sequence performances for multi spacecraft scenarios with $n = 4$. Once again, the Δv is the sum of all spacecraft Δv and the Δt corresponds to the arrival time of the last spacecraft, enabling the effective activation of the constellation. Transfer sequence 'O' outperforms all the others in terms of total Δv , while transfer sequence 'A' is the fastest.

In conclusion, the transfer design technique to DROs investigated in this paper equals the ones in Ref. [9] and outperforms the ones of Ref. [11] in terms of flight time and manoeuvres cost. Moreover, a comprehensive analysis to design multi spacecraft trajectories to build DROs constellation is proposed, leading to a number of different transfer sequences.

Table 1: Transfer sequences for the 2-spacecraft scenario.

	A	B	C	D	E	F	G	H	I	J
Δv [km/s]	9.3869	9.1533	7.4153	8.6848	8.8562	7.8242	7.4494	8.3037	10.3013	9.6127
Δt [days]	108.33	238.78	291.40	290.07	287.80	149.25	195.89	280.21	301.85	310.01

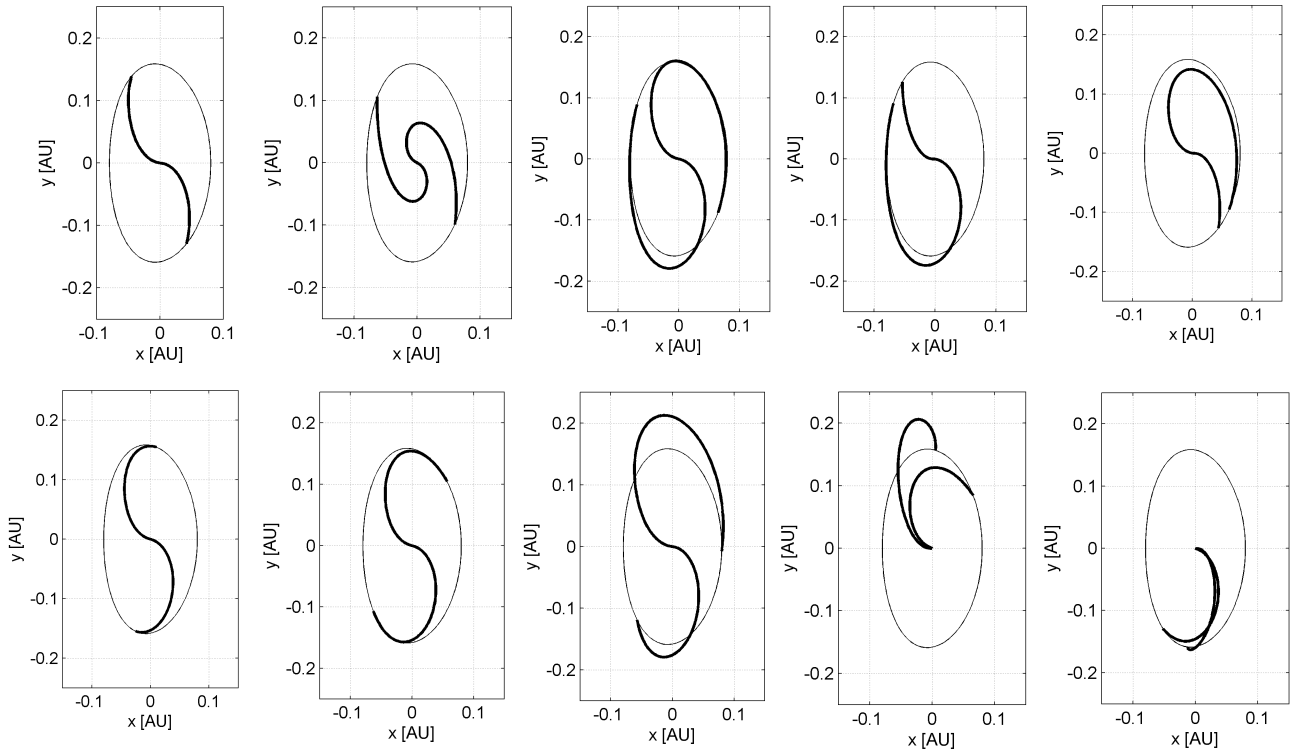

Fig. 10: Strategies for building 2 spacecraft constellation.

Table 2: Transfer sequences for the 3-spacecraft scenario.

	A	B	C	D	E	F
Δv [km/s]	13.7171	14.1513	13.0836	13.0828	14.6998	14.4660
Δt [days]	190.465	284.489	292.002	290.072	283.766	433.715

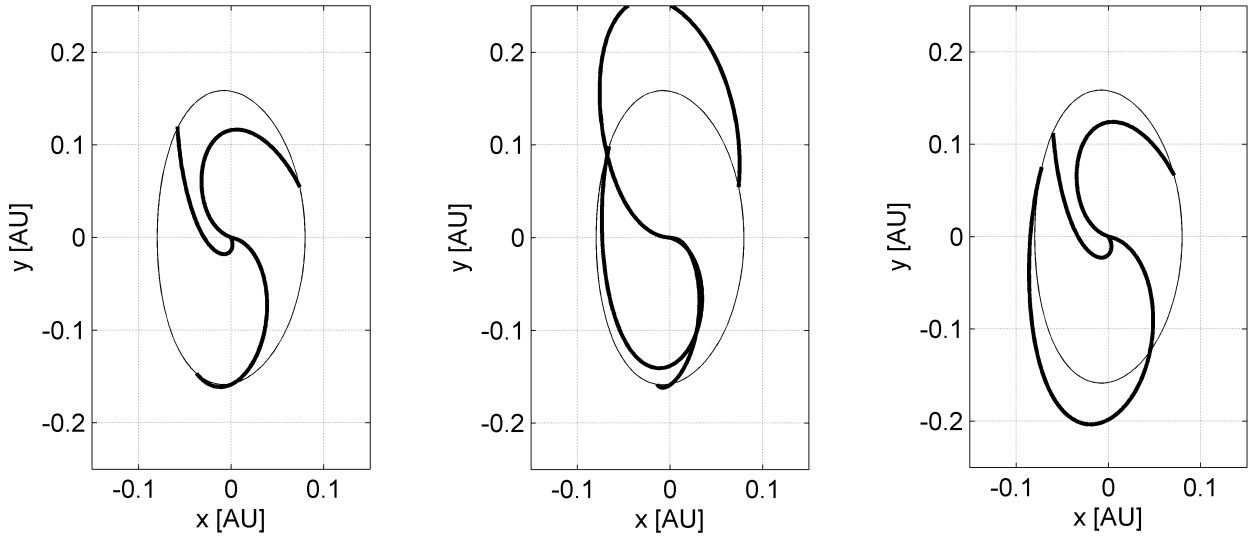

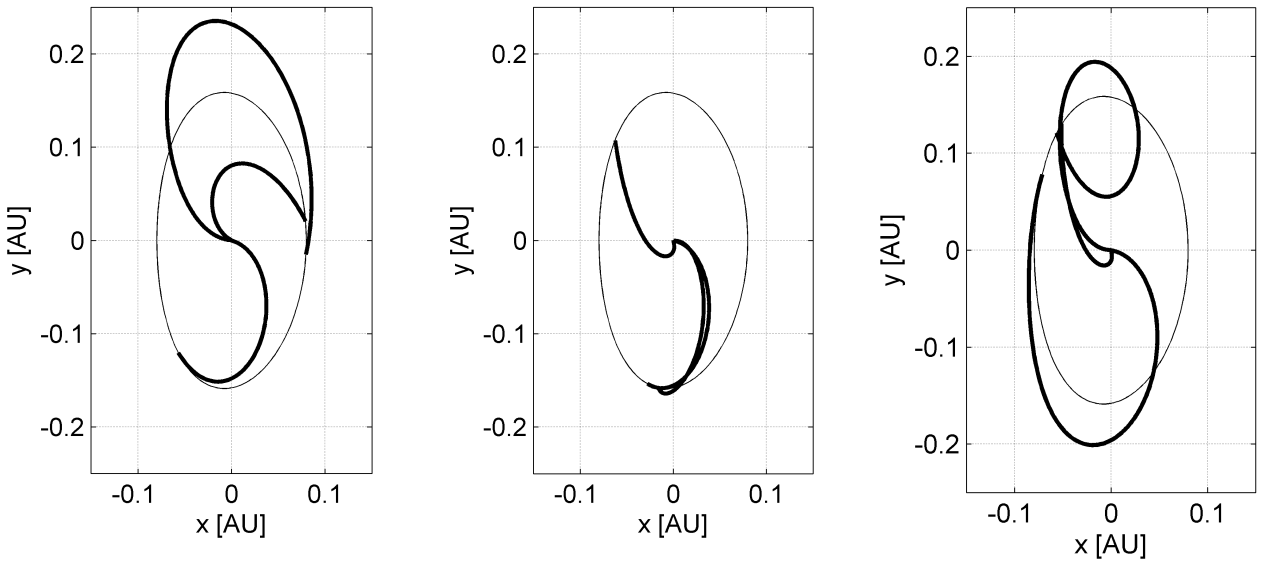

Fig. 11: Strategies for building 3 s/c constellation.

Table 3: Transfer sequences for the 4-spacecraft scenario.

	A	**B**	**C**	**D**	**E**	**F**	**G**	**H**	**I**
Δ*v* [km/s]	18.209	17.258	18.649	19.019	17.727	16.960	17.835	20.048	19.771
Δ*t* [days]	194.512	201.723	288.080	199.916	241.115	293.732	281.497	293.009	289.663
	J	**K**	**L**	**M**	**N**	**O**	**P**	**Q**	**R**
Δ*v* [km/s]	19.761	19.673	19.656	18.606	19.508	17.218	17.626	17.428	17.718
Δ*t* [days]	292.128	293.275	229.088	222.065	210.536	290.597	280.943	288.557	274.441

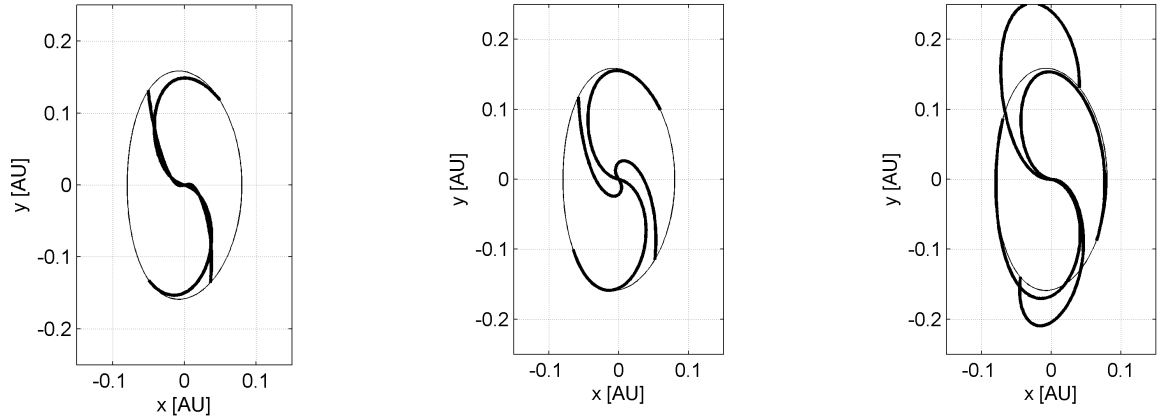

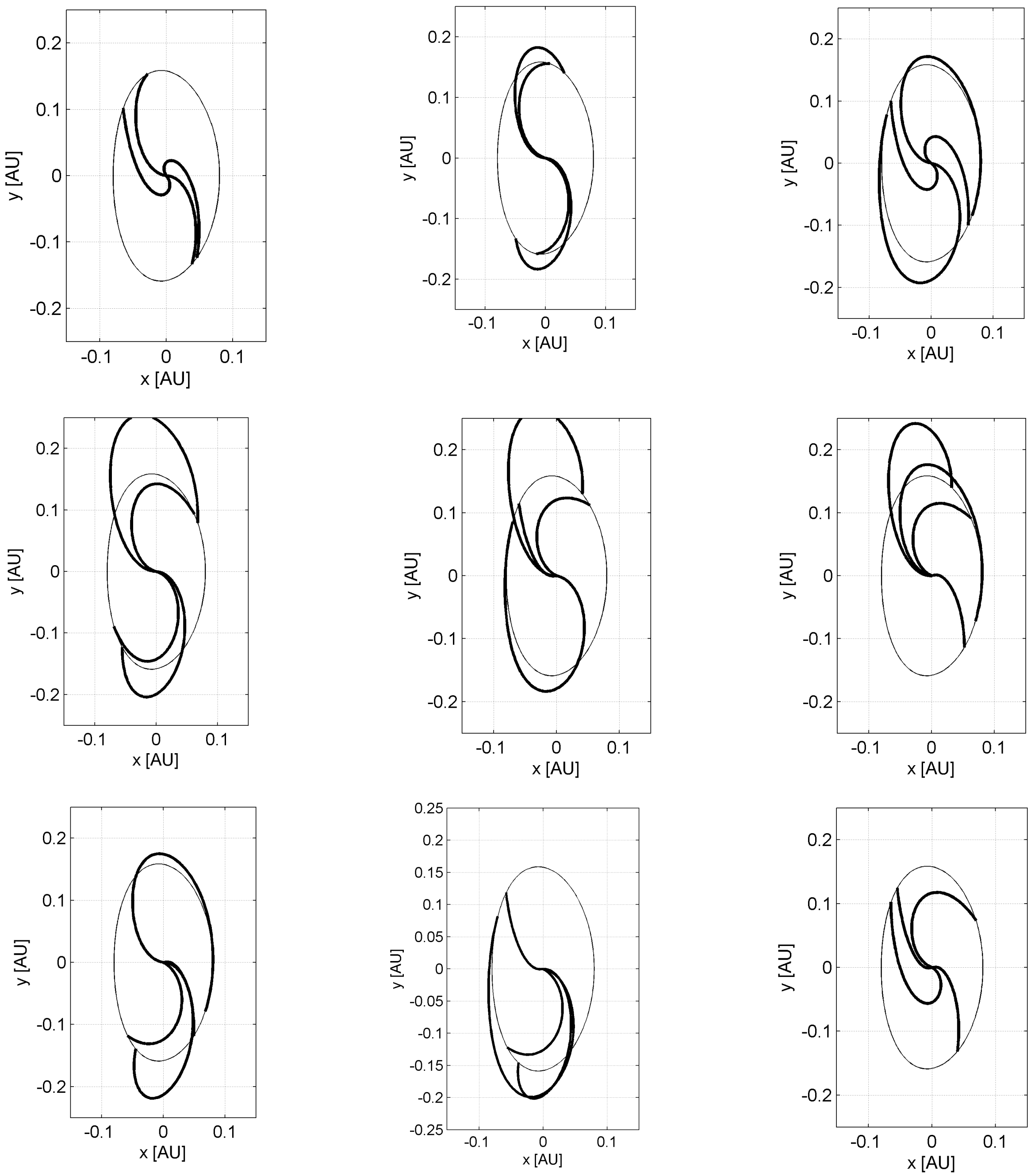
y [AU]
x [AU]

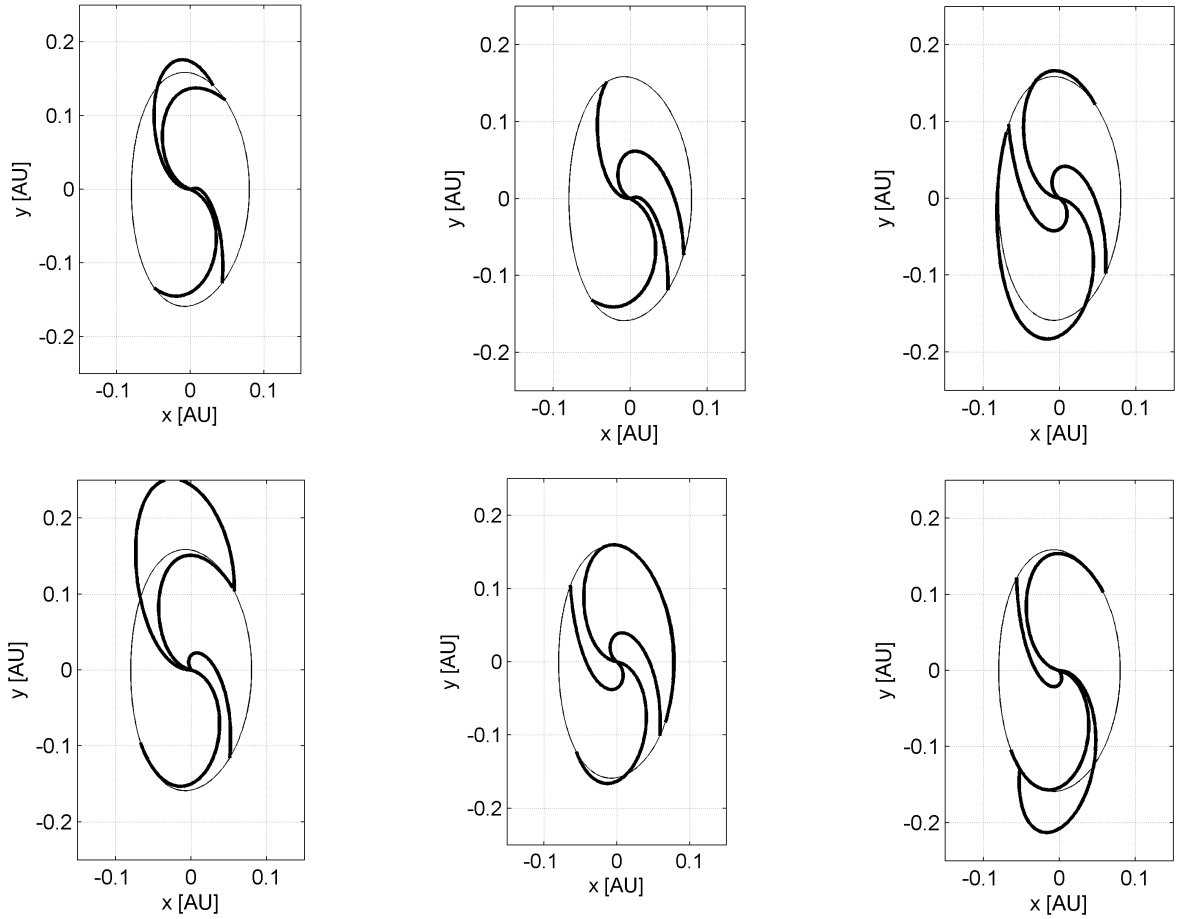

Fig. 12: Strategies for building 4 s/c constellation.

VI. CONCLUSION

This article studied the feasibility of a satellite constellation for Potentially Hazardous Asteroids. Distant Retrograde Orbits in the Sun–Earth systems are selected as they ensure increasing the warning time with respect to conventional Earth-based observation. Indeed the increase of coverage area and gained visibility in the Earth exclusion zone are demonstrated. Moreover, transfer to a selected family of DROs is designed and the strategies for building a multi-spacecraft constellation, by minimising the total required Δv to place all the spacecraft in DRO equally displaced in time. In a future work the performances of space-based observation on DROs will be also compared to the performances from a base at the L_1 point as proposed by Dunham et al. [3].

ACKNOWLEDGMENTS

The authors acknowledge Ing. Michele Stramacchia for the preliminary study of Distant Periodic Orbits for PHAs observation described in [5]. C. Colombo acknowledges the support received by the Marie Curie grant 302270 (SpaceDebECM - Space Debris Evolution, Collision risk, and Mitigation) within the 7th European Community Framework Programme. G. Mingotti and C. McInnes acknowledge the ERC Advanced Investigator Grant - 227571: VISIONSPACE, Orbital Dynamics at Extremes of Spacecraft Length-Scale.

VII. REFERENCES

[1] Stokes G.H., Yeomans D.K., Bottke D.K., Chesley S.R., Gold R.E., Evans J.B., Harris A.W., Jewitt D., Kelso D., McMillan T.S., Spahr R.S., Worden T.B., *Study to Determine the Feasibility of Extending the Search for Near-Earth Objects to Smaller Limiting Diameters*. NASA, Editor 2003.

[2] Laurin D., Hildebrand A., Cardinal R., Harvey W., Tafazoli S., "NEOSSat: A Canadian small space telescope for near Earth asteroid detection". *Proceedings SPIE 7010, Space Telescopes and Instrumentation 2008: Optical, Infrared, and Millimeter*, 701013, 12 Jul. 2008, doi:10.1117/12.789736.

[3] D. W. Dunham, H. J. Reitsema, E. Lu, R. Arentz, R. Linfield, C. Chapman, R. Farquhar, A. A. Ledkov, N. A. Eismont, E. Chumachenko, "A concept for providing warning of earth impacts by small asteroids", *Solar System Research*, July 2013, Volume 47, Issue 4, pp 315-324, Aug 2013.

[4] Sentinel Mission, web: http://b612foundation.org/sentinel-mission/ [last retrieved on 04-10-2013]

[5] Stramacchia M., Colombo C., Bernelli-Zazzera F., "Distant periodic orbits for space-based Near Earth Objects detection", *The 24th AAS/AIAA Space Flight Mechanics Meeting*, Jan. 26-30, 2014, Santa Fe, New Mexico, AAS 14-202.

[6] Jorge I. Zuluaga and I. Ferrin, "A preliminary reconstruction of the orbit of the Chelyabinsk Meteoroid", *Earth and Planetary Astrophysics*, 2013.

[7] Valsecchi G.B., Perozzi E. and Rossi A., "A space mission to detect imminent Earth impactors." Highlights of Astronomy. Vol. 16, *XXVII IAU General Assembly*, Aug. 2009.

[8] Hénon, M., *Generating Families in the Restricted Three-Body Problem. Lecture Notes in Physics*, Springer-Verlag 1997.

[9] Ocampo C.A. and Rosborough G.W., Multiple-Spacecraft Orbit-Transfer Problem: The No-Booster case. *Journal of Guidance, Control, and Dynamics*, 1999. 22(5): p. 650-657.

[10] Ocampo, C.A. and Rosborough G.W., "Transfer Trajectories for Distant Retrograde Orbiters of the Earth", *NASA STI/Recon Technical Report A*, 95 (1993): 81418.

[11] Demeyer, J. and P. Gurfil, Transfer to Distant Retrograde Orbits Using Manifold Theory. *Journal of Guidance, Control, and Dynamics*, 2007. 30(5): p. 1261-1267.

[12] Gómez, G., Koon W.S., Lo M.W., Marsden J.E., Masdemont J., and Ross S.D., "Connecting orbits and invariant manifolds in the spatial restricted three-body problem." *Nonlinearity*, Vol.17, No. 5 (2004): 1571.

[13] Koon W. S., Lo M. W., Marsden J. E., Ross S. D., *Dynamical Systems the Three-Body Problem and Space Mission design*, Marsden Books, 2005, ISBN 978-0-615-24095-4.

[14] Szebehely V., *Theory of Orbits: The Restricted Problem of Three Bodies*, 1967.

[15] Bowell, E., Hapke, B., Domingue, D., Lumme, K., Peltoniemi, J., Harris, A. W., Asteroids II, Univ. of Arizona Press, Tucson, AZ, 1989, pp. 524–556.

[16] Michelsen, R., Near-Earth Asteroids from Discovery to Characterisation, Astronomical Observatory, Niels Bohr Institute for Astronomy, *Physics and Geophysics*, 2004.

[17] Sanchez J. P., Colombo C., "Impact hazard protection efficiency by a small kinetic impactor", *Journal of Spacecraft and Rockets*, Vol. 50, No. 2, Mar.–Apr. 2013, doi: 10.2514/1.A32304.

[18] Veres, P., Jedicke, R.,Wainscoat, R., Granvik, M., Chesley, S., Abe, S., Denneau, L., and Grav, T., "Detection of Earth-Impacting Asteroids with the Next Generation All-Sky Surveys," *Icarus*, Vol. 203, No. 2, 2009, pp. 472–485. doi:10.1016/j.icarus.2009.05.010

[19] Werner, S. C., Harris, A. W., Neukum, G. and Ivanov, B. A., "The near-Earth Asteroid Size–Frequency Distribution: A Snapshot of the Lunar Impactor Size–Frequency Distribution," *Icarus*, Vol. 156, No. 1, 2002, pp. 287-290. doi: http://dx.doi.org/10.1006/icar.2001.6789.

[20] Mingotti G., Topputo F., and Bernelli-Zazzera F., "Numerical Methods to Design Low-energy, Low-thrust Sun-perturbed Transfers to the Moon." *In Proceedings of 49th Israel Annual Conference on Aerospace Sciences*, Tel Aviv-Haifa, Israel, pp. 1-14. 2009.